ELSEVIER

Journal of Volcanology and Geothermal Research 88 (1999) 1–13

Journal of volcanology and geothermal research

# Injection and arrest of dykes: implications for volcanic hazards

Agust Gudmundsson [a,*], Laura B. Marinoni [b], Joan Marti [c]

[a] *Geological Institute, University of Bergen, Allegt. 41, N-5007 Bergen, Norway*
[b] *Department of Earth Sciences, Universita degli Studi di Milano, via Mangiagalli 34, 20131 Milan, Italy*
[c] *Institute of Earth Sciences 'Jaume Almera', CSIC, Lluis Sole Sabaris s / n, 08028 Barcelona, Spain*

Received 5 January 1998; accepted 14 September 1998

**Abstract**

Dykes are the principal channels through which magma reaches the surface in volcanic eruptions. For this reason dykes observed in the field are commonly assumed to be feeders to lava flows. The actual proportion of dykes reaching the surface is, however, poorly known. In order to develop models for the purpose of estimating volcanic hazard, this proportion must be known. This follows because such models should not only consider the probability of dykes being injected from magma chambers during periods of unrest in the associated volcanoes, but also the probability of the injected dykes being arrested. This paper presents field data on several thousand dykes from Iceland and Tenerife (Canary Islands) indicating that many, and probably most, dykes become arrested at various crustal levels and never reach the surface to feed eruptions. Using the results of analytical and numerical models, it is shown that, for common loading conditions, the stress field in the vicinity of a magma chamber may favour the injection and propagation of dykes while the stress field at a certain distance from the chamber favours dyke arrest. This means that many dykes that are injected from the chamber propagate only for a very limited distance from the chamber to the point where they become arrested. The implication is that during periods of unrest in volcanoes, the probability of volcanic eruption is only a small fraction of the probability of dyke injection from the source magma chamber. 

*Keywords:* dyke injection; volcanic hazards; magma chambers; stress fields

## 1. Introduction

Most volcanic eruptions are supplied with magma through fractures. Magma-filled fractures, frozen or fluid, are referred to as dykes when they are subvertical and as sheets when they are inclined. Both dykes and inclined sheets, however, propagate as magma-filled fractures, so that there is no difference between them as regards their mechanics of emplacement. Thus, while the location, attitude and thicknesses of these two types of dykes are different (Gudmundsson, 1995), for the purpose of the present paper no distinction need be made between dykes and inclined sheets and both will be referred to as dykes.

Dyke arrest is a subject that has received little attention until very recently. Most descriptions of

* Corresponding author. Fax: +47-5558-9416; E-mail: agust.gudmundsson@geol.uib.no

0377-0273/99/$ - see front matter 
PII: S0377-0273(98)00107-3

arrested dyke tips published to date focus on lateral tips (Hoek, 1994, 1995; Rubin, 1995). In order to estimate volcanic hazard, however, it is the arrest of vertical tips of dykes approaching the earth surface (and thus potential feeder-dykes) that is of main importance. Therefore, in this paper we focus on vertical dyke tips.

One aim of this paper is to provide field data on vertically arrested dykes in Iceland and Tenerife (Canary Islands). We present detailed descriptions and measurements of the tips of selected dykes in these areas and, in addition, statistical data on the proportion of dykes being arrested. A second aim of the paper is to provide a mechanical model to explain the condition for dyke arrest. For this purpose the results of analytical and boundary-element models of the stress fields around magma chambers are presented and their consequences for dyke arrest explored.

## 2. Dyke tips

To determine the geometry and proportion of dykes that become arrested, extensive field studies of dykes, focusing on vertical dyke tips, were made in Iceland and Tenerife. The data set includes mostly basaltic dykes, ranging in age from late Tertiary to Holocene. More specifically, the set includes more than 5000 dykes in Iceland (Gudmundsson, 1995, 1998) and nearly 580 dykes in Tenerife (Marinoni and Gudmundsson, 1998).

In collecting statistical data such as those in this paper, it is important to follow clear operational rules so as to avoid as far as is possible subjective judgements. Here we have followed the rule to restrict our attention to the dykes as they appear in the profiles. Thus, dyke tips belonging to offset parts of segmented dykes that are seen to continue higher up in the profile are omitted in this data set, but no attempt was made to check if the dyke was segmented outside the profile. Similarly, the attitudes and thicknesses and tips of the dykes used here are those measured in the profiles, whereas all these parameters could be different had other profiles been available and studied. It follows that in these statistical considerations it is irrelevant (and, for most dykes, impossible to determine) whether or not other segments of a dyke seen to be arrested in a particular profile were able to reach the surface.

### 2.1. Iceland

In Iceland, the dyke tips were studied in profiles along cliffs of basaltic lava flows in mountains, river channels and on the coast (Fig. 1). Lava flows in the Tertiary and Pleistocene lava pile are generally 5–15 m thick (Saemundsson, 1979). Most profiles are along individual lava flows so that the visible vertical exposure of individual dykes that dissect the profiles are normally 5–15 m. Using the depth-dependent distribution of zeolites and other secondary minerals in Iceland (Walker, 1960, 1974; Jefferis and Voight, 1981), the estimated depths of the measured dyke profiles in the Tertiary and Pleistocene lava pile below the initial (pre-erosional) surface are from 500 m to 1000 m.

The probability that an observed dyke is seen to terminate in a profile normally increases with decreasing depth of the profile below the initial top of the lava pile. This follows because all dykes observed in vertical section through a lava pile with the topmost, pre-erosional, lava flow preserved must terminate (as feeders or non-feeders) in that section. All dykes meeting with the topmost flow, whether or not they are feeders, must terminate in that flow. Deeper in the lava pile, a dyke observed in a particular lava flow may terminate either in that flow or in any flow higher up (at shallower level) in the lava pile. Thus, as the depth of profile increases, the vertical section within which a particular dyke can terminate becomes larger and, consequently, the probability of the dyke terminating in that particular profile smaller.

From these considerations, and the data on the thicknesses and depths of the lava flows in Iceland, the minimum mathematical (a priori) probability of seeing dykes terminate vertically would be in a profile along a 5-m-thick lava flow at the depth of 1000 m below the initial top of the pile. This probability is 5/1000 or 0.5%. Similarly, the maximum mathematical probability of seeing the upper tips of dykes in a profile at 500 m depth would be 15/500 or 3%.

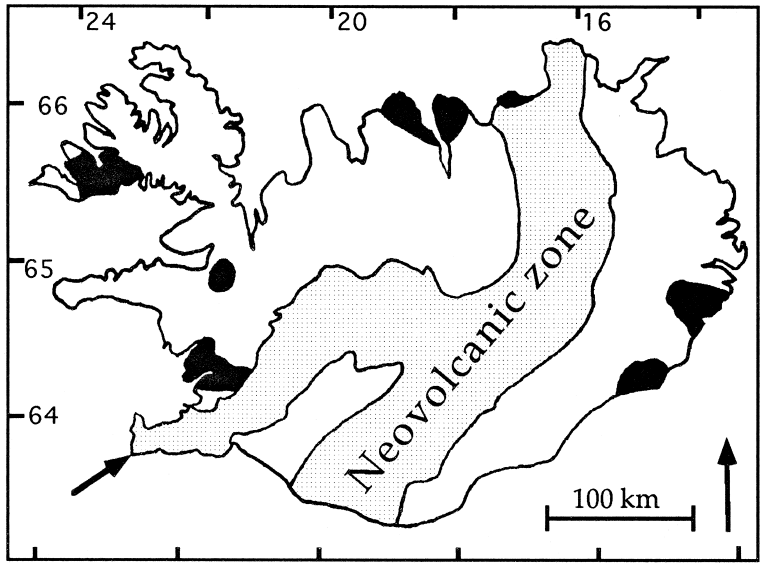


Fig. 1. Location of the main areas in Iceland (black) where late Tertiary and early Pleistocene dykes (and dyke tips) have been studied. Also shown is the neovolcanic zone, covered by rocks younger than 0.7 Ma (belonging to the Brunhes magnetic epoch), and the location of the dyke in Fig. 2 (arrow).

The field results show that, in the regional dyke swarms in Iceland, it is common that 1–3% of dykes dissecting a particular profile are observed to terminate vertically in that profile. These dyke tips became arrested at some stage during the dyke propagation, so that the observed part of the dyke never reached the surface to supply magma to a volcanic eruption.

These results indicate that the actual percentage of dykes observed to terminate in profiles in the Tertiary and Pleistocene lava pile in Iceland are within the range of the mathematical probabilities estimated above. None of the dykes observed to terminate is connected with a lava flow; all the dykes are non-feeders. Occasional feeders have been found in Iceland, but they occur outside the profiles selected for the statistical study and are mostly limited to Holocene areas (Gudmundsson, 1995). Therefore, the results suggest that the majority of dykes in Iceland terminate by simply tapering away, and that they are non-feeders.

One of the best example of a vertical dyke termination in Iceland comes from the Holocene rift zone (Fig. 2). This dyke is exposed in sea-cliffs of the Reykjanes Peninsula in Southwest Iceland. At the bottom of the profile the dyke is 0.34 m thick, but it gradually decreases in thickness towards its tip which is at only 5 m depth below the surface of the Holocene rift zone.

### 2.2. Tenerife

We have studied dykes at several places in Tenerife. Here, however, the focus is on the exceptionally well-exposed dykes measured in profiles in the peninsula of Anaga (Fig. 3). The host rock is of late Tertiary age (Ancochea et al., 1990) and consists mainly of basaltic lava flows alternating with layers of pyroclastic rocks. From the essential lack of secondary minerals in the area, and from dyke features such as vesicles, we estimate that the depth of these profiles below the top of the pre-erosional lava pile at the time of dyke emplacement does not exceed a few hundred metres.

All the profiles are along road-cuts where the explored exposure of the dykes is normally around 10 m. If the depth of these profiles was 300 m, the mathematical probability of observing dykes termi-

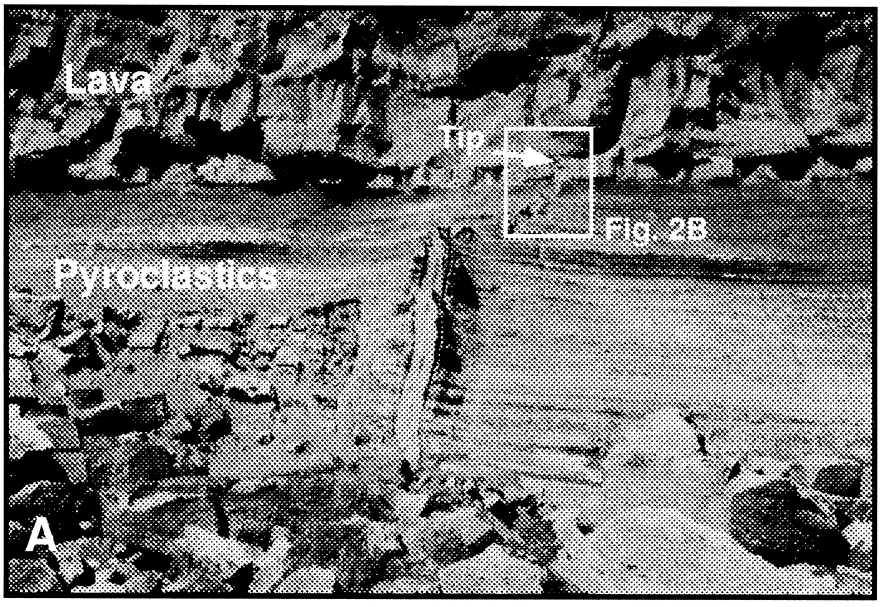
Lava
Tip
Fig. 2B
Pyroclastics
A

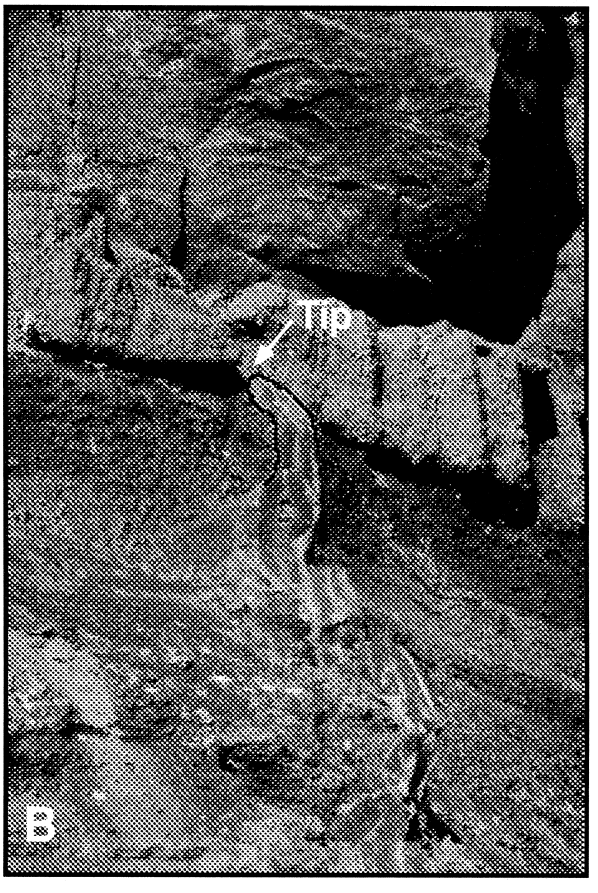
Tip
B

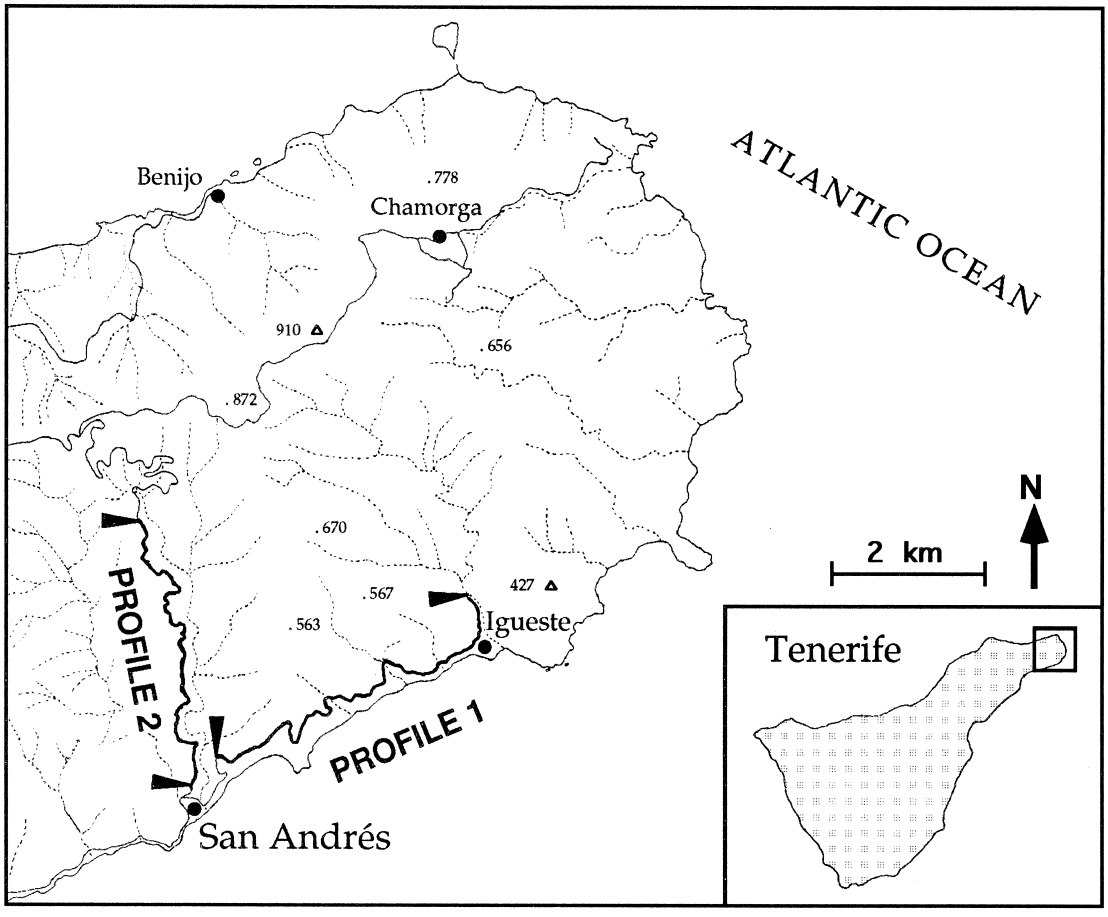


Fig. 3. Location of the two main dyke profiles in the peninsula of Anaga (Tenerife). The total number of dykes dissecting these two profiles is around 300. Elevation above sea level is in metres. On the inset map of Tenerife, the location of Anaga is indicated.

nate vertically would be 10/300 or roughly 3%; if the depth was 200 m the probability would be 5%; and if the depth was 100 m the probability would be 10%. In the profiles in Anaga, nearly 6% of the dykes were seen to terminate, indicating that the actual average depth of these profiles is 150–200 m below the surface at the time of dyke emplacement. As in Iceland, all the dykes observed to terminate vertically are non-feeders and most simply taper away so that the thickness gradually decreases towards the tip (Fig. 4).

## 3. Mechanics of dyke arrest

It has been suggested that a dyke may become arrested when flow of magma into its tip is blocked by solidification, that is, when its propagation veloc-

Fig. 2. Typical geometry of a dyke ending vertically in Iceland (located in Fig. 1). This dyke is exposed in sea-cliffs of the Holocene rift zone of Southwest Iceland. (A) View NE, at the bottom of the section the dyke thickness is 0.34 m, but gradually decreases to 0.1 m over a vertical distance of 8 m. (B) A small, offset and discontinuous segment of the dyke, mostly 9 cm thick, continues vertically up to the bottom of the 5 m thick Holocene lava flow. The margins and the tip of the uppermost part of the segment are outlined. There is no visible dyke-related faulting at the dyke tip.

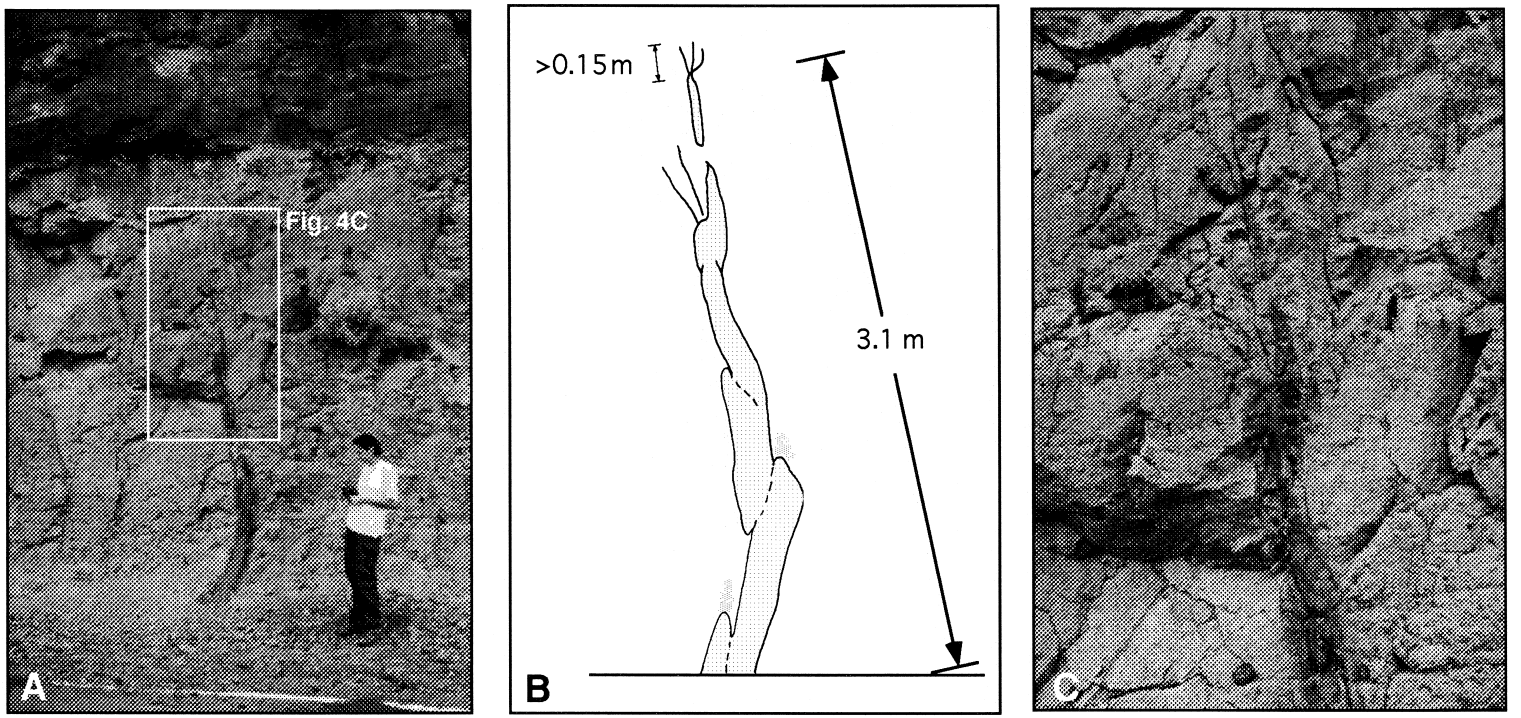


Fig. 4. Segmented dyke ending vertically in Tenerife. (A) View W, the dyke thickness gradually decreases from 0.25 m at the bottom of the exposure to around 2 cm at the dyke tip. The dyke rock is dense basalt with common vesicles, mostly 1–2 mm in diameter, and some small amygdales. The vesicles are somewhat concentrated to the centre of the dyke, but there is no clear concentration of vesicles towards the dyke tip. The pyroclastic host rock is baked next to the dyke. (B) There are three fan-shaped joints, 10–15 cm long, associated with the dyke tip. These joints may have been generated by stress concentration at the dyke tip, either during or after its emplacement. (C) Otherwise, there is no dyke-related fracturing at the dyke tip, seen here in a close-up.

ity decreases below a critical level (Delaney and Pollard, 1982; Rubin, 1993; Hoek, 1994; Lister, 1995). That model certainly needs to be considered in greater detail. One apparent difficulty, however, is to explain why the dyke should stop even if its tip became partly solidified. As long as there was any significant magmatic overpressure in the dyke, the tensile stress concentration at the dyke tip should be sufficient to rupture any solidified parts. For example, the common dip (vertical) dimension of dykes in Iceland and Tenerife may be several kilometres, whereas the radius of curvature of a typical dyke tip is only a few centimetres, suggesting potentially high tensile stress concentration at the tip of an overpressured fluid dyke. This conclusion applies of course also in cases when the magma front has a larger radius of curvature than, and does not reach to the tip of, the advancing dyke-fracture. Normally, it would be easier for the dyke to propagate through its own partly solidified tip material rather than through the solidified host rock (which would often be made of the same basaltic material as the solidified dyke tip). This follows, first, because partly solidified rock generally has lower tensile strength than completely solidified rock of the same type (Shaw, 1980) and, second, because the tensile stress concentration around the dyke would normally be greatest at or near its tip (Savin, 1961; Jaeger and Cook, 1969).

In the absence of convincing evidence for dykes being arrested primarily because of tip solidification, we are compelled to look for other models of dyke arrest. Here we explore an alternative model in which the dyke becomes arrested when its tip enters crustal layers where the dyke-normal compressive stress exceeds the magmatic pressure in the dyke.

### 3.1. Dyke injection

Tensile rupture of a magma chamber occurs when the magmatic pressure in excess of the local minimum compressive (maximum tensile) principal stress, $\sigma_3$, exceeds the tensile strength of the host rock at the boundary of the chamber. This conclusion follows from rock-mechanics considerations (Jaeger and Cook, 1969) and has been confirmed in numerous in situ hydrofracture experiments (Haimson and Rummel, 1982; Amadei and Stephansson, 1997), the tensile rupture of a pressurised drill hole being analogous to that of a magma chamber. It should be noted that the local $\sigma_3$ is, because of stress concentration around the magma chamber, normally different from the far-field, regional $\sigma_3$ (Savin, 1961; Gudmundsson, 1988). For an active (fluid) magma chamber, tensile failure of its boundary normally results in dyke injection from the chamber, provided the following condition is satisfied (Jaeger and Cook, 1969; Gudmundsson, 1990):

$$p_l + p_e = |\sigma_3| + T \qquad (1)$$

where $p_l$ is the lithostatic pressure and $p_e$ is the magmatic excess pressure above the lithostatic pressure (before dyke injection from the chamber). In this equation, both the numerical value of the minimum compressive stress $\sigma_3$ and the tensile strength $T$ of the host rock refer to their local magnitudes at the chamber boundary.

For constant tensile strength, the condition of Eq. (1) is reached when the magmatic excess pressure becomes equal to the tensile strength. This can happen when the volume of magma in the chamber increases, the minimum principal compressive stress at the boundary of the chamber decreases, or both. The tensile strength of the host rock at the boundary of an active magma chamber is normally only several mega-pascals. The in situ tensile strength of the upper part of the crust in Iceland is from 1 MPa to 6 MPa (Haimson and Rummel, 1982). Here the maximum excess magmatic pressure in the chamber before rupture, which is equal to the host-rock tensile strength, is taken as 5 MPa.

When a dyke propagates upwards into the roof of the magma chamber, the static magmatic overpressure in the dyke either increases or decreases depending on the density difference between the host rock and the magma. The static magmatic overpressure, $\Delta p$, in a vertical dyke, when compared with the minimum horizontal compressive stress $\sigma_h$ in the host rock at a certain vertical distance $h$ from the magma source chamber, is given by (Gudmundsson, 1990):

$$\Delta p = p_e + (\rho_r - \rho_m) gh + \Delta\sigma \qquad (2)$$

where $p_e$ is the magmatic excess pressure above the lithostatic pressure (before dyke injection from the

chamber), $\rho_r$ and $\rho_m$ are the densities of the host rock and the magma, respectively, $g$ is the acceleration due to gravity, and $\Delta\sigma = \sigma_v - \sigma_h$ is the difference between the vertical and the minimum horizontal compressive stress. In crustal layers where propagation of vertical dykes is favoured, the horizontal stress is normally the minimum principal compressive stress, that is, $\sigma_h = \sigma_3$. Also, in such layers, the vertical stress is commonly equal to the maximum principal compressive stress, that is, $\sigma_v = \sigma_1$. At great crustal depths, the host-rock density exceeds that of the magma, so that the overpressure in a vertically propagating dyke increases with the height of the dyke, $h$. Shallow crustal chambers, however, are commonly located in crustal layers of densities similar to that of the magma in the chambers; the density of the chamber roof is then normally less than the density of the magma (Gudmundsson, 1990). Because of degassing, the density of basaltic magma in a dyke can decrease. As observed in Hawaii, this density decrease, however, occurs only in the uppermost several hundred metres of the feeder dyke (Greenland et al., 1988). Although, at these shallow depths, the density of the host rock in an active volcanic area is also less than that at deeper levels, decrease in magma density may keep the term $(\rho_r - \rho_m)gh$ positive for some dykes at shallow depths. Commonly, however, for dykes injected from shallow magma chambers the term $(\rho_r - \rho_m)gh$ is either zero or negative.

Rupture of a magma chamber and dyke injection from it normally occurs when the stress difference $\Delta\sigma$ at the boundary of the chamber is positive. Commonly, this stress difference is generated by tensile stress concentration around the chamber which reduces $\sigma_h$ and makes $\Delta\sigma = \sigma_v - \sigma_h > 0$. At the boundary of the chamber and in its vicinity, the tensile stress is absolute (negative) but relative (reducing the compressive stress) elsewhere. As is indicated below, for many magma-chamber geometries and loading conditions, this tensile stress concentration, hence the stress difference, is limited to the immediate vicinity of the chamber. At greater distances from the chamber the tensile stress concentration normally decreases rapidly so that $\Delta\sigma \to 0$. Furthermore, previously injected dykes may, temporarily, generate stress barriers where $\sigma_h > \sigma_v$ in certain crustal layers (Gudmundsson, 1990), in which case $\Delta\sigma < 0$. This means that, on propagating from the chamber, the dyke may rapidly enter crustal layers where all the terms in the right side of Eq. (2) approach zero or become negative except the initial excess pressure $p_e$, which thereby becomes the only driving pressure that the dyke possesses. The term $p_e$ is, however, equal to the tensile strength of the host rock and normally only a few mega-pascals (Haimson and Rummel, 1982). Because of pressure drop, due to viscous drag and other factors (Rubin, 1995; Lister, 1995), the excess pressure may soon fall to zero and the dyke becomes arrested.

### *3.2. Stress fields around deep-seated magma chambers*

Consider now how the tensile stress concentration, hence (for a vertical dyke) the stress difference $\Delta\sigma$, decreases from the boundary of a magma chamber. The far-field stress variation around a spherical magma chamber of radius $a$ located at great depth (relative to its radius) below the surface can be modelled using a centre-of-dilatation nucleus of strain

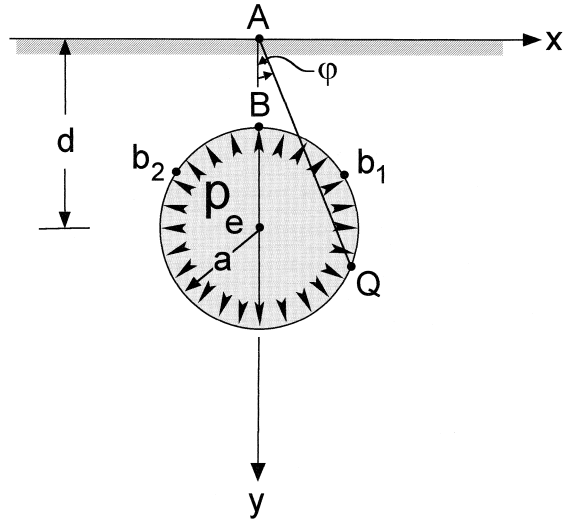


Fig. 5. Magma chamber of circular vertical cross section subject to internal magmatic excess pressure, $p_e$, as the only loading. The chamber has radius $a$ and its centre is at depth $d$ below the free surface of the earth. The maximum tensile stress at the boundary occurs where the angle $\varphi$ reaches a maximum, namely at points $b_1$ and $b_2$ (where AQ is tangent to the boundary of the chamber). Point A is at the surface above the centre of the chamber; (B) is the point on the chamber boundary that is next to the free surface.

in a full space. If the chamber is subject to internal magmatic excess pressure $p_e$ as the only loading, the radial, $\sigma_r$, and the tangential, $\sigma_\theta$, stresses in the rock hosting the chamber are (Jaeger and Cook, 1969):

$$\begin{aligned} \sigma_r &= p_e(a/r)^3 \\ \sigma_\theta &= -\frac{p_e}{2}(a/r)^3 \end{aligned} \quad (3)$$

where $r$ is the radius-vector from the origin to a point in the host rock. The radial stress is compressive and considered positive, whereas the tangential stress is tensile and considered negative. If $a \to 0$ in Eq. (3) but $p_e a^3$ is finite, the intensity $S$ or the strength of the nucleus if given by the equation:

$$S = p_e a^3 \quad (4)$$

Eqs. (3) and (4) show that the intensity $S$ of the local stress field around the spherical magma chamber falls off inversely as the cube of the distance from the chamber. Thus, simultaneously, the stress conditions for dyke injection and propagation, as presented in Eq. (1), may be satisfied in the immediate vicinity of the chamber but not at some greater distance from the chamber. A dyke propagating upwards from the chamber may thus be arrested in crustal layers at a certain distance from the chamber.

### 3.3. Stress fields around shallow magma chambers

Eqs. (3) and (4) apply to a relatively deep-seated spherical magma chamber subject to internal excess pressure as the only loading. For shallow magma chambers subject to different loading conditions, simple analytical results are not available and the solutions for the stress fields must be obtained by numerical methods.

For a shallow crustal magma chamber of circular vertical cross section, that is, a cylindrical chamber with a horizontal long (infinite) axis, with radius $a$ and depth to its centre $d$, subject to an internal magmatic excess pressure $p_e$ (Fig. 5) the tensile stress along its boundary, $\sigma_b$, is given by (Savin, 1961):

$$\sigma_b = p_e(1 + 2\tan^2\varphi) \quad (5)$$

where the angle $\varphi$ is as defined in Fig. 5. The tensile stress at the boundary of the chamber reaches a maximum at points $b_1$ and $b_2$ (where AQ is tangent

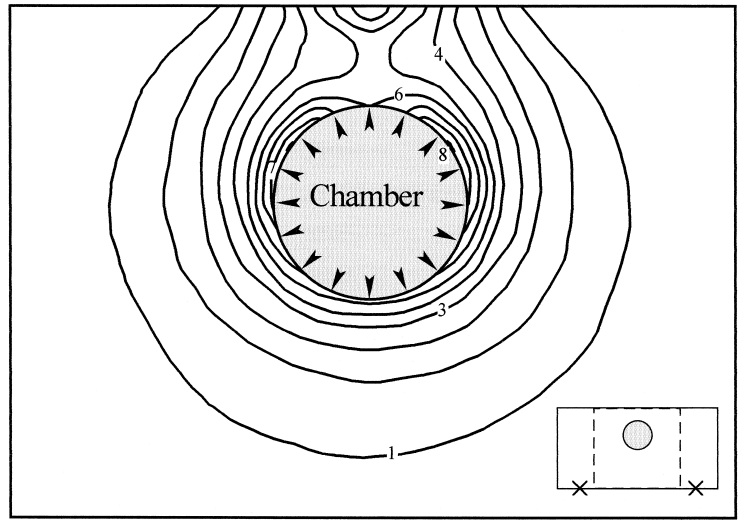


Fig. 6. Boundary-element results showing the stress field around a magma chamber of circular vertical cross-section subject to internal magmatic excess pressure of 5 MPa as the only loading. The contours show the magnitude of the maximum principal tensile stress $\sigma_3$ in mega-pascals. The whole model is shown on the inset. The crosses indicate approximately the boundary condition of no displacement in the model, and the broken lines outline the parts for which the stress fields are presented.

to the boundary of the magma chamber), where the angle $\varphi$ is maximum, and is given by:

$$\sigma_{b,max} = \frac{p_e(d^2 + a^2)}{d^2 - a^2} \quad (6)$$

If $d > 1.73a$ the maximum tensile stress at the boundary of the chamber, at points $b_1$ and $b_2$, is greater than the maximum tensile stress at the free surface, which occurs at point A (Fig. 5). Otherwise, the tensile stress at the surface is the greatest. The tensile stress at point B, the point at the boundary of the chamber that is next to the free surface, is equal to the excess magmatic pressure in the chamber $p_e$, but at points A, $b_1$ and $b_2$, the magnitude of the tensile stress depends on the ratio $d/a$. When the value of $a$ approaches that of $d$, the theoretical magnitude of the tensile stress can become many times greater than the normal magmatic excess pressure $p_e$. Eq. (1) indicates, however, that the actual tensile stress at these points cannot exceed the tensile strength of the host rock and should, therefore, normally be only several mega-pascals.

Consider now the general stress field in the vicinity of a magma chamber similar to that in Fig. 5. For that purpose, the BEASY (1991) boundary-element program was used to calculate the local stresses around the chamber. The shapes that were considered most likely to exist during the activity of the chamber are a sphere and an oblate spheroid (sill-like chamber). The models explored here are two-dimensional (one horizontal axis being infinite), but the results compare very well with known three-dimensional (and two-dimensional) analytical results for stress fields around cavities and holes (Savin, 1961; Tsuchida and Nakahara, 1970; Tsuchida et al., 1982).

The chamber is modelled as a hole subject to (1) positive excess pressure and (2) no internal excess pressure but remote tensile stress (plate pull). Before these loadings (driving stresses) are applied, the chamber is assumed to be in lithostatic equilibrium with the host rock so that the state of stress is isotropic (hydrostatic). A lithostatic state of stress is generated by the weight of a column of the overburden of unit area and thus includes the acceleration due to gravity (Jaeger and Cook, 1969). The litho-

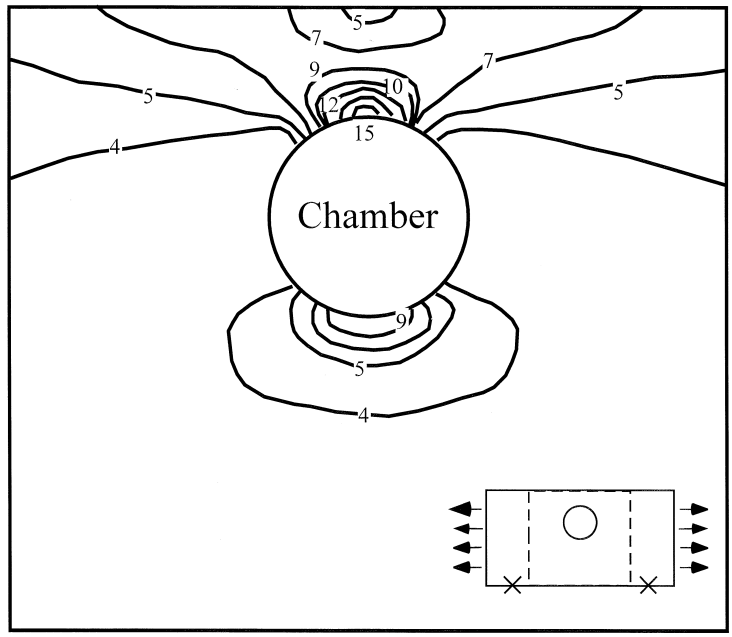


Fig. 7. Boundary-element results showing the stress field around a magma chamber of circular vertical cross section subject to remote horizontal tensile stress (plate pull) of 5 MPa as the only loading. The contours show the magnitude of the maximum principal tensile stress $\sigma_3$ in mega-pascals. The whole model is shown on the inset.

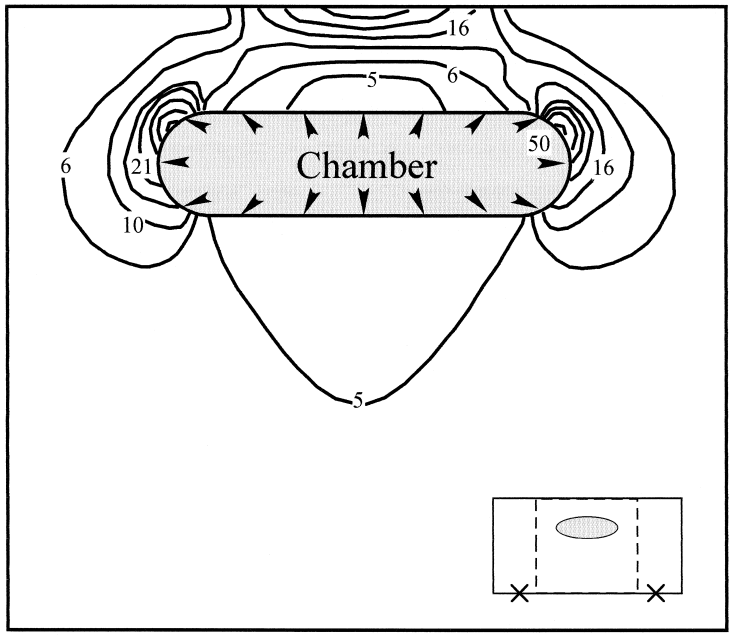


Fig. 8. Boundary-element results on the stress field around a sill-like magma chamber subject to internal magmatic excess pressure of 5 MPa as the only loading. The contours show the magnitude of the maximum principal tensile stress $\sigma_3$ in mega-pascals. The whole model is shown on the inset.

sphere containing the magma chamber and the associated volcano is modelled as a semi-infinite elastic plate. The static Young's modulus of the elastic plate is 40 GPa and Poisson's ratio is 0.25; these values are appropriate for a basaltic crust (Gudmundsson, 1988), but the results are not very sensitive to changes in the elastic moduli.

For a magma chamber of circular vertical cross-section subject to internal magmatic excess pressure $p_e$ of 5 MPa as the only loading, the highest tensile stress concentration occurs at the boundary of the chamber (Fig. 6) in the areas marked by points $b_1$ and $b_2$ in Fig. 5. We also considered a magma chamber of circular cross-section that is initially in lithostatic equilibrium and is then subjected to remote horizontal tensile stress (plate pull) of 5 MPa as the only loading. In this case, the highest tensile stress concentration occurs at the boundary of the chamber that is next to the free surface (Fig. 7).

A sill-like chamber subject to horizontal tensile stress has little effect on the regional rift-zone stress field (Savin, 1961). For a sill-like magma chamber subject to internal magmatic excess pressure $p_e$ of 5 MPa as the only loading, however, the results (Fig. 8) are generally similar to those of a spherical magma chamber subject to the same loading conditions (Fig. 6); the highest tensile stress concentration at the boundary of the chamber occurs at its marginal parts.

The boundary-element results for all these magma-chamber geometries and loading conditions show that the intensity of the tensile stress field falls off rapidly with distance from the boundary of the chamber. Thus, during periods of unrest in a volcano, the stress field near the source magma chamber commonly satisfies Eq. (1) and gives rise to dyke injection from the chamber while at a certain distance the terms $\Delta\sigma$ and $(\rho_r - \rho_m)gh$ in Eq. (2) are zero or negative, and the term $p_e$ approaches zero, so that the dyke becomes arrested.

## 4. Discussion

The probability of an eruption in a volcano during periods of unrest is of vital importance in estimating volcanic hazard and, eventually, in assessing the

volcanic risk for the area surrounding the volcano. The analytical and numerical results, together with the field observations, presented in this paper indicate that dyke arrest may frequently occur as a result of the dyke entering crustal layers where the dyke-normal compressive stress exceeds the magmatic excess pressure at the dyke tip. The implication is that many, and perhaps most, dykes injected from magma chambers during periods of unrest in volcanoes do not reach the surface, but become arrested at various crustal depths. This conclusion is supported by the observation that most episodes of unrest in volcanoes do not lead to volcanic eruption (Newhall and Dzurisin, 1988).

The analytical and numerical results, as presented by Eqs. (3) and (4) and in Figs. 6–8, show that the rapidity with which the tensile stress associated with the magma chamber falls off with distance from the chamber depends on the chamber geometry and loading conditions. The most rapid fall-off is in the case of a deep-seated spherical chamber subject to internal excess pressure as the only loading (Eqs. (3) and (4)), whereas the stress intensity of a sill-like chamber subject to the same loading falls off more slowly. In this model, the faster the rate of decrease of the tensile stress with distance from the chamber, the greater is the probability of dykes from the chamber being arrested.

This conclusion is based on the generalised stress fields around magma chambers modelled as cavities (cf. Gudmundsson, 1998). But there are other factors that can contribute to dykes becoming arrested. For example, stress barriers, that is, layers where the minimum horizontal compressive stress is greater than the vertical stress, may be common in rift zones (Gudmundsson, 1990) and elsewhere (Amadei and Stephansson, 1997). When a propagating dyke meets with a stress barrier of this kind, the dyke may change into a sill or propagate laterally beneath the barrier; alternatively, the dyke may become arrested (Gudmundsson, 1990).

These results demonstrate the importance of knowing roughly the geometry and the loading conditions of magma chambers in order to estimate volcanic hazards. The loading conditions can commonly be deduced from the tectonic regime within which the magma chamber is located. The geometry of the chamber, however, is normally more difficult to determine with certainty. Seismic tomography provides some information on the geometry (Gudmundsson et al., 1994), but is usually not sufficiently accurate for the purpose of the present stress-field calculations. A general numerical model on the geometrical evolution of magma chambers in different thermo-tectonic environments is clearly needed. The test-implications of such a model could be checked by field data on the upper parts of the deeply eroded magma chambers (plutons) of extinct central volcanoes.

## Acknowledgements

This work was supported by the EC contract number ENV4-CT96-0259, and by grants from the Iceland Science Foundation (to AG), from Consiglio Nazionale delle Ricerche (to LBM), and from CICYT AMB96-0498-C04 (to JM).

## References

Amadei, B., Stephansson, O., 1997. Rock Stress and Its Measurement. Chapman and Hall, London.

Ancochea, E., Fuster, J.M., Ibarrola, E., Cendrero, A., Coello, J., Hernan, F., Cantagrel, J.M., Jamond, C., 1990. Volcanic evolution of the island of Tenerife (Canary Islands) in the light of new K–Ar data. J. Volcanol. Geotherm. Res. 44, 231–249.

BEASY, 1991. The Boundary Element Analysis System User Guide. Computational Mechanics Publications, Southampton.

Delaney, P., Pollard, D.D., 1982. Deformation of host rocks and flow of magma during growth of minette dikes and breccia-bearing intrusions near Ship Rock, New Mexico. U.S. Geol. Surv. Prof. Pap. 1202, 1–61.

Greenland, L.P., Okamura, A.T., Stokes, J.B., 1988. Constraints on the mechanics of the eruption. In: Wolfe, E.W. (Ed.), The Puu Oo Eruption of Kilauea Volcano, Hawaii: Episodes 1 Through 20, January 3, 1983 Through June 8, 1984. U.S. Geol. Surv. Prof. Pap. 1463, pp. 155–164.

Gudmundsson, A., 1988. Effect of tensile stress concentration around magma chambers on intrusion and extrusion frequencies. J. Volcanol. Geotherm. Res. 35, 179–194.

Gudmundsson, A., 1990. Emplacement of dikes, sills and crustal magma chambers at divergent plate boundaries. Tectonophysics 176, 257–275.

Gudmundsson, A., 1995. Infrastructure and mechanics of volcanic systems in Iceland. J. Volcanol. Geotherm. Res. 64, 1–22.

Gudmundsson, A., 1998. Magma chambers modeled as cavities explain the formation of rift zone volcanoes and their eruption and intrusion statistics. J. Geophys. Res. 103, 7401–7412.

Gudmundsson, O., Brandsdottir, B., Menke, W., Sigvaldason, G.E., 1994. The crustal magma chamber of the Katla volcano in south Iceland revealed by 2D seismic undershooting. Geophys. J. Int. 119, 277–296.

Haimson, B.C., Rummel, F., 1982. Hydrofracturing stress measurements in the Iceland research drilling project drill hole at Reydarfjördur, Iceland. J. Geophys. Res. 87, 6632–6649.

Hoek, J.D., 1994. Mafic Dykes of the Vestfold Hills, East Antarctica. An Analysis of the Emplacement Mechanism of Tholeiitic Dyke Swarms and of the Role of Dyke Emplacement During Crustal Extension. Ph.D. Thesis, University of Utrecht, Utrecht.

Hoek, J.D., 1995. Dyke propagation and arrest in Proterozoic tholeiitic dyke swarms. Vestfold Hills, East Antarctica. In: Baer, G., Heimann, A. (Eds.), Physics and Chemistry of Dykes. Balkema, Rotterdam, pp. 79–93.

Jaeger, J.C., Cook, N.G.W., 1969. Fundamentals of Rock Mechanics. Methuen, London.

Jefferis, R.G., Voight, B., 1981. Fracture analysis near the mid-ocean plate boundary, Reykjavik–Hvalfjördur area, Iceland. Tectonophysics 76, 171–236.

Lister, J.R., 1995. Fluid-mechanical models of the interaction between solidification and flow in dykes. In: Baer, G., Heimann, A. (Eds.), Physics and Chemistry of Dykes. Balkema, Rotterdam, pp. 115–124.

Marinoni, L.B., Gudmundsson, A., 1998. Dyke emplacement in shield-stage formations of Tenerife. Ann. Geophys. 16, C189, Supplement.

Newhall, C.G., Dzurisin, D., 1988. Historical unrest at large calderas of the world. US Geol. Surv. Bull. 1855, 1–1108.

Rubin, A.M., 1993. On the thermal viability of dikes leaving magma chambers. Geophys. Res. Lett. 20, 257–260.

Rubin, A.M., 1995. Propagation of magma-filled cracks. Annu. Rev. Earth Planet. Sci. 8 (23), 287–336.

Saemundsson, K., 1979. Outline of the geology of Iceland. Jökull 29, 7–28.

Savin, G.N., 1961. Stress Concentration Around Holes. Pergamon Press, New York.

Shaw, H.R., 1980. The fracture mechanisms of magma transport from the upper mantle. In: Hargraves, R.B. (Ed.), Physics of Magmatic Processes. Princeton University Press, Princeton, pp. 201–264.

Tsuchida, E., Nakahara, I., 1970. Three-dimensional stress concentration around a spherical cavity in a semi-infinite elastic body. Japan Soc. Mech. Eng. Bull. 13, 499–508.

Tsuchida, E., Saito, Y., Nakahara, I., Kodama, M., 1982. Stresses in a semi-infinite body containing a prolate spheroidal cavity subjected to an axisymmetric pressure. Japan Soc. Mech. Eng. Bull. 25, 891–897.

Walker, G.P.L., 1960. Zeolite zones and dike distribution in relation to the structure of the basalts of eastern Iceland. J. Geol. 68, 515–527.

Walker, G.P.L., 1974. The structure of eastern Iceland. In: Kristjansson, L. (Ed.), Geodynamics of Iceland and the North Atlantic Area. D. Reidel, Norwell, pp. 177–188.